Chemical Science

ROYAL SOCIETY OF CHEMISTRY

EDGE ARTICLE

View Article Online
View Journal | View Issue

Cite this: *Chem. Sci.*, 2024, **15**, 19604

All publication charges for this article have been paid for by the Royal Society of Chemistry

Received 5th September 2024
Accepted 5th November 2024

DOI: 10.1039/d4sc06012a

rsc.li/chemical-science

CuBr-mediated surface-initiated controlled radical polymerization in air†

Menglu Chen,[a] Shuai You,[a] Tingting Guo,[b] Haohao Ren,[b] Longzu Zhu,[a] Peize Wang,[a] Wenbo Sheng, *[b] Chenliang Gong *[a] and Wei Li *[a]

Herein, we present a straightforward CuBr-mediated surface-initiated controlled radical polymerization (SI-CRP) method for fabricating polymer brushes using microliter volumes of reaction solution in air and at room temperature. The key advantage of this method is its ability to rapidly grow polymer brushes with oxygen tolerance, driven by the controlled disproportionation of Cu^{I} into Cu^{II} and Cu^{0} by CuBr and ligand. We demonstrate the successful preparation of homo-, block, patterned, and wafer-scale polymer brushes. Additionally, the catalyst in CuBr-mediated SI-CRP is reusable, long-lasting, and compatible with various monomers. This work broadens the potential of CuBr for polymer brush growth, making it accessible to both experts and non-experts.

Introduction

Surface-initiated reversible deactivation radical polymerization (SI-RDRP), also called surface-initiated controlled radical polymerization (SI-CRP) techniques have become major in surface modification by polymer brushes with controlled compositions, architectures, and functionalities.[1,2] Surface-initiated atom transfer radical polymerization (SI-ATRP) is one of the most popular and powerful SI-CRP techniques.[3] SI-ATRP uses transition metal halide (commonly copper) complexes formed with amine-containing ligands to mediate the equilibrium between the active radicals and dormant organic halide species (Fig. 1a).[4] $Cu^{I}X/L$ is the activator that reacts with the initiator, generating radicals and $Cu^{II}X/L$. The radicals can start the polymerization and react with $Cu^{II}X/L$ to get $Cu^{I}X/L$ and a dormant chain with a halogen group. Conventional SI-ATRP typically involves relatively large amounts of $Cu^{I}X/L$ catalyst, high polymerization temperature, stringent anaerobic conditions (such as in a glove box or by freeze–pump–thaw method), and tedious polymerization time, only yielding thin polymer brushes.[5–8]

To address these limitations, various new SI-ATRP techniques mediated by reducing agents,[9–11] electrochemical chemistry,[12–14] photochemistry,[15,16] and zerovalent metal (*e.g.* Cu,[7,17–22] Zn,[23–25] Fe,[26,27] Sn[28]) have been developed. The key characteristic of these methods is the reduction of metal halide from a higher oxidation state to a lower oxidation state to start surface-initiated polymerization.[29] These methods use minimal amounts of the catalyst and can be performed at room temperature. Another attractive advantage of these methods is that they eliminate the need for external deoxygenation, allowing polymerization to occur without it. The main reason for omitting the deoxygenation process is that oxygen in the reaction system can be consumed by oxidizing Cu^{I} species into Cu^{II} species.[30] Recently, Anastasaki *et al.* reported using low ppm CuBr to trigger ATRP at ambient temperature with simple

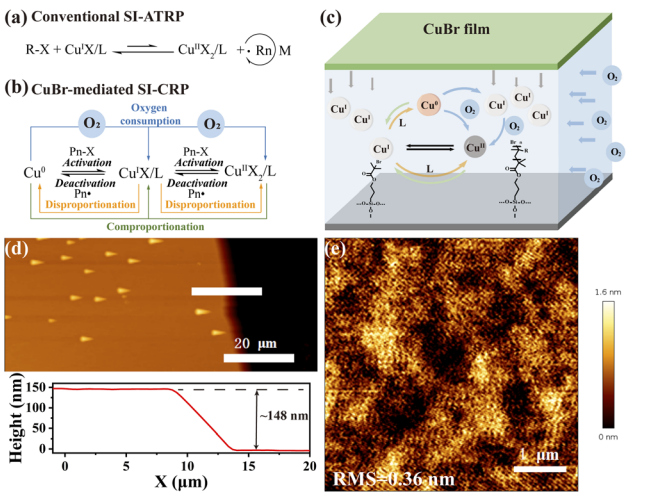

Fig. 1 (a) The mechanism of conventional SI-ATRP. Schematic illustrating the mechanism (b) and assembly setup (c) of CuBr-mediated SI-CRP under ambient conditions. (d) AFM image and the corresponding height profile of PSPMA brushes by CuBr-mediated SI-CRP. (e) AFM image (scan area 5 × 5 μm^2) of PSPMA brushes.

[a]State Key Laboratory of Applied Organic Chemistry, College of Chemistry and Chemical Engineering, Lanzhou University, Lanzhou 730000, P. R. China. E-mail: w_li@lzu.edu.cn; gongchl@lzu.edu.cn

[b]State Key Laboratory of Solid Lubrication, Lanzhou Institute of Chemical Physics, Chinese Academy of Sciences, Lanzhou 730000, P. R. China. E-mail: shengwb@licp.cas.cn

† Electronic supplementary information (ESI) available. See DOI: https://doi.org/10.1039/d4sc06012a

nitrogen bubbling.[8] Haddleton reported *in situ* disproportionation of Cu^{I}-assisted CRP under both sealed and open-air conditions through a two-step process.[31] Their approach further demonstrated that the catalyst widely used in conventional ATRP is also effective in solution polymerization with some oxygen tolerance at room temperature. However, they both involved tedious processes and tris-(2-(dimethylamino) ethyl)amine as the ligand that is expensive and needs stepwise synthesis.

Inspired by the above, herein, we explore the potential of CuBr to facilitate the synthesis of polymer brushes in air and at ambient temperature, termed CuBr-mediated SI-CRP. This method is shown to be oxygen-tolerant and user-friendly, using microliter volumes of the reaction solution to realize multiple polymer brush growth on a wafer scale under ambient conditions with high-end group fidelity. The prepared CuBr films show high stability and reusability and can also be used to prepare patterned polymer brushes.

Results and discussion

To verify the practicability of CuBr-mediated SI-CRP, a typical procedure for CuBr-mediated SI-CRP is shown in Scheme S1.† CuBr films are prepared by coating CuBr and poly(methyl methacrylate) (PMMA) on a cover glass. CuBr films exhibit two key features: one is to control the diffusion of CuBr into the reaction solution and the other is as an oxygen barrier to hinder oxygen into the reaction system. The cleaned silicon wafer modified with α-bromoisobutyrate initiator and the as-prepared CuBr film on a cover glass were assembled into a sandwich structured device with a gap that is filled by the reaction solution containing monomer, ligand and solvent (Fig. 1c). A cost-friendly *N*,*N*,*N*′,*N*″,*N*″-pentamethyldiethylenetriamine (PMDETA) is chosen as the ligand and the hydrophilic SPMA is selected as the monomer. They are dissolved in a solvent (methanol : water = 0.5 : 1) and a microliter volume of the reaction solution is added to the setup mentioned above under ambient conditions. After the reaction for a certain time, the substrate is thoroughly cleaned and dried for further characterization. A significant reduction in the contact angle of the silicon wafer after polymer brush growth indicates successful surface modification (Scheme S1†). The presence of the peaks of the S–O stretch at 1050 cm^{-1} and S=O stretch at 1150 cm^{-1} in the infrared spectroscopy (IR) image (Fig. S1a†) further confirmed the formation of polymer brushes. The atomic force microscopy (AFM) test shows that the PSPMA brushes with a thickness of around 148 nm (Fig. 1d) are obtained and exhibit a homogeneous morphology, with a low root mean square roughness (RMS) of about 0.36 nm (Fig. 1e). Besides PMMA, polydimethylsiloxane (PDMS) and porous CuBr film can also work for polymer brush growth (Fig. S3†). The above results confirm that CuBr can be successfully used to prepare polymer brushes in air.

To further elucidate the mechanism of CuBr-mediated SI-CRP, we first test the effects of CuBr amount on the polymer brush growth. Different CuBr films were prepared by mixing varying amounts of CuBr with PMMA onto a cover glass, and the results are shown in Fig. 2a. When CuBr film prepared from 0.01 g is used, there is almost no polymer brush growth. With increasing the amount of CuBr, the thickness of polymer brushes first reaches a summit with a value of about 124 nm and then shows a two-stage fall-off. Three typical points marked with bright color (Fig. 2a) ($CuBr_{0.025}$/$CuBr_{0.1}$/$CuBr_{0.5}$) are selected for further investigation. The actual content of CuBr in the films is calculated (detailed information can be found in the ESI†). The amount of CuBr per unit area for the three typical points is 0.31, 0.99, and 4.94 μmol cm^{-2}, respectively (Table S1†).

The ligand dosage affects CuBr-mediated SI-CRP differently (Fig. 2b). For $CuBr_{0.025}$, 1 μL and 5 μL of PMDETA result in almost no polymer brush growth. As the PMDETA dosage increases, the thickness of the polymer brushes rises with a maximum of about 200 nm with 10 μL of PMDETA, then decreases with further increases in PMDETA. For $CuBr_{0.1}$, the thickness of the polymer brushes surges to a maximum of 165 nm from 1 to 5 μL of PMDETA, then decreases with additional PMDETA. When using $CuBr_{0.5}$, the thickness of the polymer brushes consistently decreases with increasing PMDETA. Due to the limited solubility of CuBr in water, the addition of PMDETA can enhance the formation of the Cu^{I} complexes soluble in the reaction medium. The soluble Cu^{I} complexes can be disproportionate into Cu^{0} and Cu^{II} species alongside the rapid consumption of oxygen.[31] The ratio of Cu^{I}, Cu^{0} and Cu^{II} control the polymer brush growth. Varying the concentration of PMDETA will affect the amount of the soluble Cu^{I} complexes which will have a great effect on the disproportionation/comproportionation equilibrium (Fig. 1b),

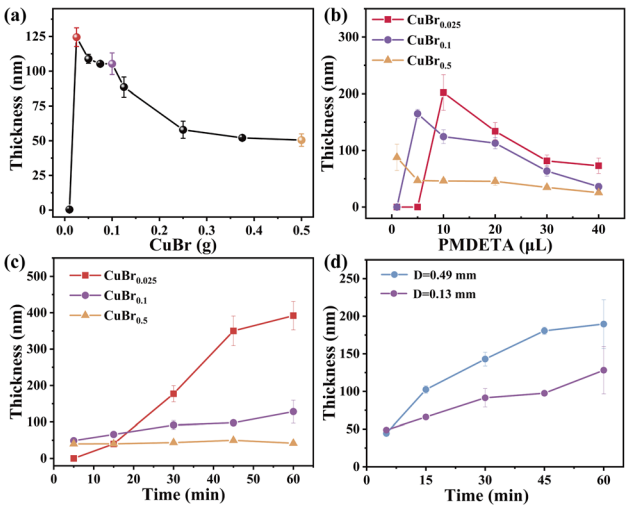

Fig. 2 (a) Comparison of PSPMA brushes *via* CuBr-mediated SI-CRP by varying CuBr amounts. $CuBr_x$ represents the CuBr prepared by *x* g of CuBr (PMDETA 20 μL, polymerization time 30 min). (b) Influence of the PMDETA amount on the SI-ATRP of CuBr-mediated SI-CRP using $CuBr_{0.025}$/$CuBr_{0.1}$/$CuBr_{0.5}$ (polymerization time for 30 min, D = 0.13 mm). (c) The growth kinetics of PSPMA brushes *via* $CuBr_{0.025}$/$CuBr_{0.1}$/$CuBr_{0.5}$, respectively (PMDETA 10 μL, D = 0.13 mm). (d) Comparison of PSPMA brushes *via* CuBr-mediated SI-CRP at D = 0.13 mm and D = 0.49 mm.

resulting in different ratios of Cu^{I}, Cu^{0} and Cu^{II}, and consequently brush thicknesses.

Reaction kinetics is an effective way to reflect the controllability of the reaction and explain the mechanism. Thus, we compared the kinetics of CuBr-mediated SI-CRP using $CuBr_{0.025}$, $CuBr_{0.1}$, and $CuBr_{0.5}$ as catalysts at the spacing of 0.13 mm (Fig. 2c). When $CuBr_{0.025}$ is used as the catalyst, there is an induction period of 5 min and a nearly linear increase of the PSPMA brush thickness with time from 5 to 45 min, showing its controllability. Then the growth rate of the polymer brushes slows down after 45 min. When $CuBr_{0.1}$ is used as the catalyst, the increase of CuBr amount relative to $CuBr_{0.025}$ enhances the oxygen consumption capacity of the reaction system, which makes the result that about 50 nm-thick polymer brush can be obtained in 5 min. The thickness of the polymer brush also increases linearly with time while the growth rate is much lower than that of $CuBr_{0.025}$, which may be due to the Cu^{II} species as the deactivators in the system rise relative to $CuBr_{0.025}$ and inhibit the reaction. When $CuBr_{0.5}$ is used as the catalyst, the thickness of the polymer brush hardly changes with reaction time. There are two possible explanations: (i) the high concentration of radicals generated by a high concentration of CuBr and the following radical termination; (ii) the high concentration of Cu^{II} species formed from the disproportionation of CuBr inhibits the reaction. To further prove the reason, the end-group fidelity is tested. We prepared two PSPMA brushes with $CuBr_{0.5}$ after polymerization for 30 and 60 min. We then try to do the *in situ* growth on these two PSPMA brushes to check if we can make diblock polymer brushes. The results are shown in Fig. S4† and diblock homopolymer brushes are obtained successfully under both conditions, which supports the second explanation. We also compared the grafting densities of polymer brushes with $CuBr_{0.025}$, $CuBr_{0.1}$, and $CuBr_{0.5}$ according to the previous report[32–34] and the results are shown in Table S2.† $CuBr_{0.025}$ gives the lowest grafting density while $CuBr_{0.1}$ gives the highest followed by $CuBr_{0.5}$, indicating that CuBr can control the grafting density of polymer brushes *via* CuBr-mediated SI-CRP. The reason for the lowest grafting density of $CuBr_{0.025}$ is that the long polymer chains obtained by a fast polymerization rate can prevent the free monomers from getting close to the neighboring initiator surface.[35,36] In addition, the CuBr films before and after polymerization were characterized by X-ray diffraction (XRD) and the results are shown in Fig. S1b.† Compared with CuBr before polymerization, a new small peak at $2\theta = 43°$ for CuBr films after polymerization appears, which is attributed to the formation of Cu^{0} *via* the disproportionation of CuBr.

Based on the above, a possible mechanism for CuBr-mediated SI-CRP in air is proposed: In the presence of a ligand, CuBr and ligand can form Cu^{I} complexes that can easily dissolve into the reaction solution. Afterward, the disproportionation of the dissolved $Cu^{I}Br/L$ complexes into Cu^{0} and Cu^{II} complexes takes place to get the disproportionation/comproportionation equilibrium that can be controlled by CuBr and ligand, and oxygen in the system can be rapidly consumed by oxidization of Cu^{I} complexes and Cu^{0}. The resulting $Cu^{I}Br/L$, $Cu^{II}Br/L$ and Cu^{0} as well as ligands take part in the controlled polymer brush growth, and their roles in this process might be similar to the previous report.[37]

The influence of oxygen on the polymer-brush growth by CuBr-mediated SI-CRP using $CuBr_{0.1}$ is further explored. The distance (D) between the initiator and CuBr film is the most common means of adjusting oxygen in the system. Therefore, the thickness of PSPMA brushes at different distances was investigated (Fig. S5†). With increasing D, the thickness of PSPMA brushes increases first, reaches a maximum value of about 195 nm at $D = 0.49$ mm and then decreases, which is mainly attributed to the influence of oxygen on Cu^{I}, Cu^{0} and Cu^{II} species involved in the mechanism for CuBr-mediated SI-CRP. Then, we compared the kinetics of CuBr-mediated SI-CRP using $CuBr_{0.1}$ under $D = 0.13$ mm and 0.49 mm (Fig. 2d). Interestingly, after a 5 minutes reaction, the thicknesses of the PSPMA brushes at $D = 0.13$ mm and 0.49 mm are similar. No induction period appears indicating that oxygen consumption proceeds rapidly. With increasing the reaction time, the thicknesses of PSPMA brushes increase at both $D = 0.13$ mm and 0.49 mm and the thickness at $D = 0.49$ mm is thicker than that at $D = 0.13$ mm. At a larger distance, more oxygen is present in the reaction system leading to the oxidization of Cu^{I} species into Cu^{II} species. The increase in Cu^{II} species can shift the disproportionation/comproportionation equilibrium toward comproportionation, enabling Cu^{I} species to initiate the polymer brush growth. The above results also demonstrate the excellent oxygen tolerance of CuBr-mediated SI-CRP.

Next, the end-group fidelity of polymer brushes synthesized by CuBr-mediated SI-CRP is examined. POEGMA brushes were synthesized and then used for the second polymer brush growth by using the same monomer (Fig. 3a, left). The resulting polymer brushes were characterized by AFM and the thickness of each layer is 94 and 37 nm shown in Fig. 3b. Besides homogeneous polymer brushes using the same monomer, diblock polymer brushes using two monomers (OEGMA and SPMA) can also be prepared (Fig. 3a, right). The resulting thicknesses of the diblock polymer brushes measured by AFM are shown in Fig. 3c. The thicknesses of POEGMA and PSPMA brushes are about 30 and 81 nm, respectively. Meanwhile, the water contact angles of the block polymer brush changed obviously with each polymerization, further showing CuBr-mediated SI-CRP with high end-group fidelity.

To further illustrate the versatility of our method, we tested the range of monomers, reusability, and stability of the CuBr films. A variety of hydrophilic monomers including ionic, acrylate, and acrylamide monomers and hydrophobic monomers including methyl methacrylate (MMA), methyl acrylate (MA) and *tert*-butyl methacrylate (*t*BuMA) (Fig. S6†) were successful for polymerization. The thicknesses of the various polymer brushes after polymerization are shown in Fig. 3d. Among them, PNIPAM brushes show the most outstanding reaction efficiency for up to ~306 nm in 30 min polymerization. Besides, the CuBr film shows high stability and can be reused for SI-CRP. We conducted CuBr-mediated SI-CRP five times using the same CuBr film and the results are shown in Fig. 3e. The thickness of PSPMA brushes is about 125 nm for the first use and almost unchanged for five uses. We also compared the

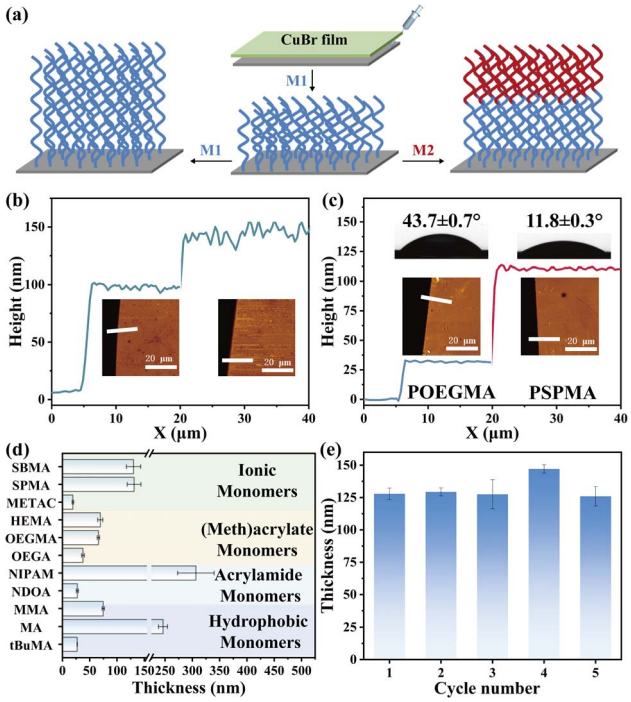

Fig. 3 (a) Schematic illustrating *in situ* chain growth of polymer brushes and preparation of diblock polymer brushes. The height analysis obtained by AFM of homo- (b) and block (c) polymer brushes. (d) Polymer brush thicknesses obtained by CuBr-mediated SI-CRP using $CuBr_{0.1}$ for 30 min with ionic, (meth)acrylate, acrylamide and hydrophobic monomers. (e) Reusability testing of $CuBr_{0.1}$ in CuBr-mediated SI-CRP.

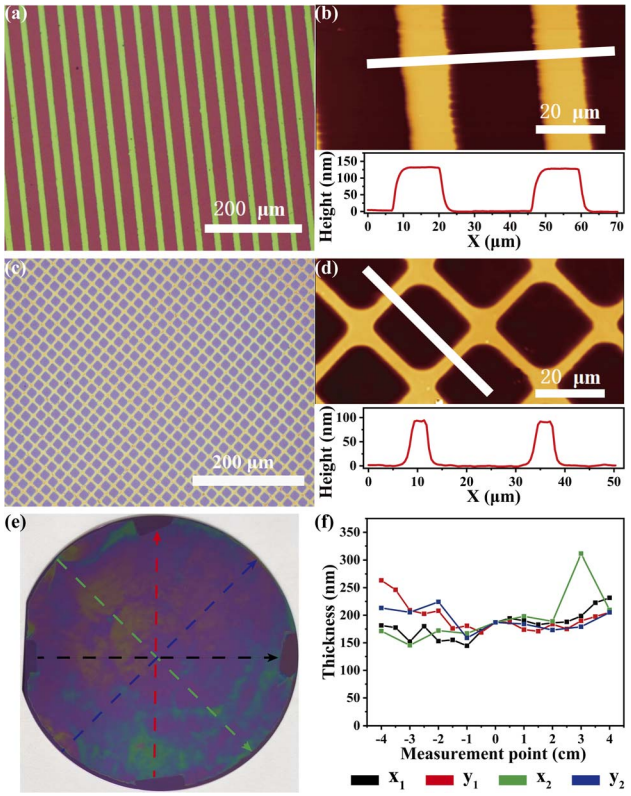

Fig. 4 Fabrication of patterned and wafer-scale polymer brushes by CuBr-mediated SI-CRP. Optical micrographs (a) and the AFM image (b) of the strip-patterned POEGMA brushes. Optical micrographs (c) and the AFM image (d) of the positive grid-patterned PSPMA brushes on the 4-inch wafer (polymerization time for 60 min, PMDETA 10 μL, D = 0.49 mm). (f) The thickness of PSPMA brushes measured by ellipsometry along radial lines corresponding to the color line in (e).

thickness of polymer brushes using the CuBr films stored on different days (Fig. S7†). Even after 80 and 100 days of placement, the catalytic effect of CuBr film did not decrease. The above results show that CuBr-mediated SI-CRP is robust.

Furthermore, CuBr-mediated SI-CRP is an attractive way to create microscopic or large-sized patterned polymer brushes. After photoresist and UV irradiation treatment through a photomask (ESI†), patterned initiator-modified substrates can be successfully prepared. After CuBr-mediated SI-CRP, the patterned polymer brush with stripe and grid shapes can be obtained and clearly shown by optical micrographs (Fig. 4a and c) and AFM images (Fig. 4b and d). In the AFM images and the corresponding height profiles, the thicknesses of patterned brushes with stripe and grid shapes are about 130 nm and 90 nm, respectively (Fig. 4b and d). Large-sized patterned positive PSPMA brushes can be also obtained by CuBr-mediated SI-CRP (Fig. S8†). To further expand the application of our method, we tried to use CuBr-mediated SI-CRP to prepare polymer brushes on the 4-inch wafer under ambient conditions. The obtained PSPMA brushes on the wafer are shown in Fig. 4e. Even at a spacing of 0.49 mm, the polymer brush area covers almost the entire wafer except where the spacers are and the ~2 mm rim at the wafer edge. The rim could be caused by air spreading into the solution.[18] According to the thicknesses of polymer brushes measured at different points on the four axes of the wafer by ellipsometry (Fig. 4f), the average brush thickness is around 180 nm. The success of this experiment bodes well for its potential to generate polymer brushes over large areas.

Conclusions

In summary, we demonstrate an oxygen-tolerant CuBr-mediated SI-CRP where the catalyst CuBr is stable and reusable. This method allows for the rapid synthesis of various polymer brushes with patterned and block architectures over large areas using minimal reaction solution in air. The high oxygen tolerance is attributed to the dissolved Cu^{I} complexes and their disproportionated products Cu^{0}. The combined roles of Cu^{I}, Cu^{0}, Cu^{II} species and the ligand are crucial for controlled polymer brush growth. The polymer brushes produced by our method exhibit high end-group fidelity and can be finely tuned by adjusting the amounts of CuBr and ligand. This approach enhances the potential of CuBr for the efficient preparation of polymer brushes and supports the development of polymer brush-based functional materials.

Data availability

The data supporting this article have been included as part of the ESI.†

Author contributions

W. L. and W. S. managed and directed the overall project and supervised the experimental work. M. C. performed the experiments. S. Y., T. G., H. R., L. Z. and P. W. do the characterization and some data collection. W. L., C. G. and W. S. co-wrote the manuscript with input from M. C. All the authors discussed the results and commented on the manuscript.

Conflicts of interest

There are no conflicts to declare.

Acknowledgements

The authors gratefully acknowledge the financial support from the National Natural Science Foundation of China (52205232) and the Natural Science Foundation of Gansu Province (24JRRA467). This work was also supported by Talent Scientific Fund of Lanzhou University.

References

1 C. W. Pester, H.-A. Klok and E. M. Benetti, *Macromolecules*, 2023, **56**, 9915–9938.
2 J. O. Zoppe, N. C. Ataman, P. Mocny, J. Wang, J. Moraes and H.-A. Klok, *Chem. Rev.*, 2017, **117**, 1105–1318.
3 Y. Zhang, M. Li, B. Li and W. Sheng, *Langmuir*, 2024, **40**, 5571–5589.
4 F. Lorandi, M. Fantin and K. Matyjaszewski, *J. Am. Chem. Soc.*, 2022, **144**, 15413–15430.
5 C. Boyer, N. A. Corrigan, K. Jung, D. Nguyen, T. K. Nguyen, N. N. Adnan, S. Oliver, S. Shanmugam and J. Yeow, *Chem. Rev.*, 2016, **116**, 1803–1949.
6 W. Li, W. Sheng, E. Wegener, Y. Du, B. Li, T. Zhang and R. Jordan, *ACS Macro Lett.*, 2020, **9**, 328–333.
7 D. Wu, W. Li and T. Zhang, *Acc. Chem. Res.*, 2023, **56**, 2329–2340.
8 R. Whitfield, K. Parkatzidis, K. G. E. Bradford, N. P. Truong, D. Konkolewicz and A. Anastasaki, *Macromolecules*, 2021, **54**, 3075–3083.
9 K. Matyjaszewski, H. Dong, W. Jakubowski, J. Pietrasik and A. Kusumo, *Langmuir*, 2007, **23**, 4528–4531.
10 G. J. Dunderdale, C. Urata, D. F. Miranda and A. Hozumi, *ACS Appl. Mater. Interfaces*, 2014, **6**, 11864–11868.
11 L. A. Navarro, A. E. Enciso, K. Matyjaszewski and S. Zauscher, *J. Am. Chem. Soc.*, 2019, **141**, 3100–3109.
12 B. Li, B. Yu, W. T. Huck, W. Liu and F. Zhou, *J. Am. Chem. Soc.*, 2013, **135**, 1708–1710.
13 B. Li, B. Yu, W. T. Huck, F. Zhou and W. Liu, *Angew. Chem., Int. Ed.*, 2012, **51**, 5092–5095.
14 N. Shida, Y. Koizumi, H. Nishiyama, I. Tomita and S. Inagi, *Angew. Chem., Int. Ed.*, 2015, **127**, 3994–3998.
15 J. E. Poelma, B. P. Fors, G. F. Meyers, J. W. Kramer and C. J. Hawker, *Angew. Chem., Int. Ed.*, 2013, **125**, 6982–6986.
16 W. Yan, S. Dadashi-Silab, K. Matyjaszewski, N. D. Spencer and E. M. Benetti, *Macromolecules*, 2020, **53**, 2801–2810.
17 W. Li, W. Sheng, B. Li and R. Jordan, *Angew. Chem., Int. Ed.*, 2021, **60**, 13621–13625.
18 W. Yan, M. Fantin, N. D. Spencer, K. Matyjaszewski and E. M. Benetti, *ACS Macro Lett.*, 2019, **8**, 865–870.
19 T. Zhang, Y. Du, F. Müller, I. Amin and R. Jordan, *Polym. Chem.*, 2015, **6**, 2726–2733.
20 D. Hafner and R. Jordan, *Polym. Chem.*, 2020, **11**, 2129–2136.
21 M. Fantin, S. N. Ramakrishna, J. Yan, W. Yan, M. Divandari, N. D. Spencer, K. Matyjaszewski and E. M. Benetti, *Macromolecules*, 2018, **51**, 6825–6835.
22 T. Zhang, E. M. Benetti and R. Jordan, *ACS Macro Lett.*, 2019, **8**, 145–153.
23 J. Yan, B. Li, B. Yu, W. T. Huck, W. Liu and F. Zhou, *Angew. Chem., Int. Ed.*, 2013, **52**, 9125–9129.
24 R. Faggion Albers, W. Yan, M. Romio, E. R. Leite, N. D. Spencer, K. Matyjaszewski and E. M. Benetti, *Polym. Chem.*, 2020, **11**, 7009–7014.
25 C. Zhang, L. Wang, D. Jia, J. Yan and H. Li, *Chem. Commun.*, 2019, **55**, 7554–7557.
26 A. Layadi, B. Kessel, W. Yan, M. Romio, N. D. Spencer, M. Zenobi-Wong, K. Matyjaszewski and E. M. Benetti, *J. Am. Chem. Soc.*, 2020, **142**, 3158–3164.
27 X. Yin, D. Wu, H. Yang, J. Wang, R. Huang, T. Zheng, Q. Sun, T. Chen, L. Wang and T. Zhang, *ACS Macro Lett.*, 2022, **11**, 693–698.
28 D. Wu, X. Yin, Y. Zhao, Y. Wang, D. Li, F. Yang, L. Wang, Y. Chen, J. Wang, H. Yang, X. Liu, F. Liu and T. Zhang, *ACS Macro Lett.*, 2023, **12**, 71–76.
29 R. Wang, Q. Wei, W. Sheng, B. Yu, F. Zhou and B. Li, *Angew. Chem., Int. Ed.*, 2023, **62**, e202219312.
30 G. Szczepaniak, L. Fu, H. Jafari, K. Kapil and K. Matyjaszewski, *Acc. Chem. Res.*, 2021, **54**, 1779–1790.
31 E. Liarou, Y. Han, A. M. Sanchez, M. Walker and D. M. Haddleton, *Chem. Sci.*, 2020, **11**, 5257–5266.
32 R. Jordan, A. Ulman, J. F. Kang, M. H. Rafailovich and J. Sokolov, *J. Am. Chem. Soc.*, 1999, **121**, 1016–1022.
33 Y. Che, T. Zhang, Y. Du, I. Amin, C. Marschelke and R. Jordan, *Angew. Chem., Int. Ed.*, 2018, **57**, 16380–16384.
34 W. Li, W. Sheng, R. Jordan and T. Zhang, *Polym. Chem.*, 2020, **11**, 6971–6977.
35 H. Liu, M. Li, Z.-Y. Lu, Z.-G. Zhang and C.-C. Sun, *Macromolecules*, 2009, **42**, 2863–2872.
36 E. Mastan, L. Xi and S. Zhu, *Macromol. Theory Simul.*, 2016, **25**, 220–228.
37 J. Lyu, Y. Miao, Z. Li, Y. Li, Y. Gao, M. Johnson, H. Tai and W. Wang, *Polymer*, 2023, **280**, 126055.